Low specific contact resistivity to graphene achieved by AuGe/Ni/Au and annealing process*

Shu-Zhen Yu(于淑珍)[1,†], Yan Song(宋焱)[1,2], Jian-Rong Dong(董建荣)[1], Yu-Run Sun(孙玉润)[1], Yong-Ming Zhao(赵勇明)[1,3], and Yang He(何洋)[1,3]

[1] *Key Laboratory of Nanodevices and Applications, Suzhou Institute of Nano-Tech and Nano-Bionics, Chinese Academy of Sciences, Suzhou* 215123, *China*

[2] *Nano Science and Technology Institute, University of Science and Technology of China, Suzhou* 215123, *China*

[3] *University of Chinese Academy of Sciences, Beijing* 100049, *China*

(Received 19 May 2016; revised manuscript received 2 August 2016; published online 30 September 2016)

Low metal–graphene contact resistance is important in making high-performance graphene devices. In this work, we demonstrate a lower specific contact resistivity of $Au_{0.88}Ge_{0.12}$/Ni/Au–graphene contact compared with Ti/Au and Ti/Pt/Au contacts. The rapid thermal annealing process was optimized to improve AuGe/Ni/Au contact resistance. Results reveal that both pre- and post-annealing processes are effective for reducing the contact resistance. The specific contact resistivity decreases from 2.5×10^{-4} to 7.8×10^{-5} Ω·cm^2 by pre-annealing at 300 °C for one hour, and continues to decrease to 9.5×10^{-7} Ω·cm^2 after post-annealing at 490 °C for 60 seconds. These approaches provide reliable means of lowering contact resistance.

Keywords: graphene, AuGe/Ni/Au, annealing, contact resistance

PACS: 81.05.ue, 73.40.Ns, 61.72.Bb **DOI:** 10.1088/1674-1056/25/11/118101

1. Introduction

Graphene made by the chemical vapor deposition technique (CVD-graphene) has been used to make ever increasing electronic devices.[1–7] Low metal–graphene contact resistance plays an important role in making high-performance graphene devices. Metal material, device processing, and graphene pattern (top and edge contact configurations) are three major factors determining the contact resistance.[8–11] Device processing including graphene transfer and lithography usually introduces contaminations such as polymethylmethacrylate (PMMA) and lithography resists. Various methods have been used, such as low-power O_2 plasma treatment, low density inductive coupled Ar plasma, and ultraviolet (UV)/O_3 treatment to clean the graphene surface.[12–14] Parameters should be tuned very carefully in order to avoid the defects introduced by these methods. Thus thermal annealing before and after metal deposition (pre-annealing and post-annealing) is more frequently used to reduce the contact resistance although the assumption that surface contamination sandwiched between the metal–graphene contact is removed during post-annealing is still controversial.[15–17]

In recent years, metal contacts Cu, Ag, Pd, and Au and metal schemes contacts Ti/Au, Cr/Au, Ni/Au, and Ti/Pt/Au have been studied.[8,10–12,18,19] Results reveal that Ti/Au and Ti/Pt/Au can provide relatively low contact resistance after O_2 plasma treatment, thermal annealing, or end- (or edge-) contact configuration. In this paper, we first compared the specific contact resistivities for Ti/Au, Ti/Pt/Au, and AuGe/Ni/Au top contacts using the circular transmission line method (CTLM). Then rapid thermal annealing (RTA) processes before and after metal deposition (pre-annealing and post-annealing) were studied for improving the metal–graphene contact resistance. Results show that AuGe/Ni/Au–graphene contact has the lowest specific contact resistivity among the Ti/Au–, Ti/Pt/Au–, and AuGe/Ni/Au–graphene contacts. Finally, the metal/graphene contact is discussed from the viewpoints of chemisorption of metal on graphene, contact area, metal work function, and surface contamination.

2. Experiments

Monolayer graphene sheets used in this work were grown by the chemical vapor deposition (CVD) method on Cu foils (Hefei Vigon Material Technology Company) and transferred onto 300 nm SiO_2/Si substrates by the polymethylmethacrylate (PMMA) method in which 100 g $CuSO_4$ + 500 mL HCl + 500 mL H_2O were used as the etching solution. In the circular transmission line method (CTLM) measurements, circular patterns with an outer radius of 110 μm and gap spacings of 5, 10, 15, 20, 25, and 30 μm were adopted. CTLM patterns were fabricated by laser lithography using LOR 20B and AZ5214 double layer photoresists which can produce a clean graphene surface following the standard lithography process.[10] Then the metal contacts Ti/Au (20/150 nm), Ti/Pt/Au (50/50/200 nm), and

*Project supported by the National Natural Science Foundation of China (Grant No. 61376065) and the Science and Technology Project of Suzhou, China (Grant No. ZXG2013044).

†Corresponding author. E-mail: szyu2010@sinano.ac.cn

© 2016 Chinese Physical Society and IOP Publishing Ltd

$Au_{0.88}Ge_{0.12}$/Ni/Au (35/10/200 nm) were deposited by an e-beam evaporator. The optical image of the CTLM patterns is shown in Fig. 1. Pre-annealing at 200 and 300 °C for 1 hour in nitrogen atmosphere was conducted using a commercial rapid thermal annealing system (RTA) to remove the residual PMMA on the graphene surface before the laser lithography and metal deposition. Furthermore, RTA post-annealing at 300–550 °C was performed to improve the metal/graphene contacts. Then electrical characterizations were carried out in air by a Keithley 4200 semiconductor parameter analyzer.

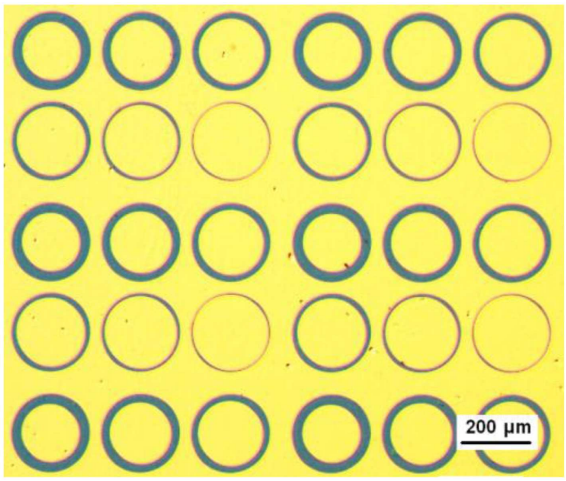


Fig. 1. Optical microscope image of the fabricated metal–graphene CTLM patterns on 300 nm SiO_2/Si substrate.

3. Results and discussion

Figure 2(a) shows the measured total resistance of each circular as a function of $\ln(R/r)$ and the linear fitting for AuGe/Ni/Au–graphene contact post-annealed at 490 °C for 15 min. In CTLM, the total resistance R_t between different gap spacings is determined as follows:[20]

$$R_t = \frac{R_{sh}}{2\pi} \times \left[\ln\left(\frac{R}{r}\right) + L_t\left(\frac{1}{r} + \frac{1}{R}\right)\right], \tag{1}$$

where R_{sh} is the sheet resistance, R and r are the outer and inner radii, and $L_t = (\rho_c/R_{sh})^{1/2}$ is the transmission line length. According to Eq. (1), R_t can be formulated as follows: $R_t = k\ln(R/r) + b$, where k is the slope of the fitted line, b is the intercept of the fitted line with the vertical axis

$$\frac{R_{sh}}{2\pi} = k, \quad \frac{R_{sh}}{2\pi} \times \left[L_t\left(\frac{1}{r} + \frac{1}{R}\right)\right] = b. \tag{2}$$

Thus the general equation for specific contact resistivity (ρ_c) calculation can be obtained by

$$\rho_c = \frac{\pi R^2 b^2}{2k}. \tag{3}$$

Figure 2(b) shows the ρ_c as a function of post-annealing conditions for Ti/Au graphene and AuGe/Ni/Au graphene contacts without pre-annealing. The ρ_c is 1.3×10^{-3} Ω·cm^2 for Ti/Au contact before post-annealing. It reduces by 7.7% and 15.4% after post-annealing at 300 °C for 1 h and at 300 °C for 1 min with 10 cycles, respectively, while it reduces by 93.8% after post-annealing at 490 °C for 15 min. The ρ_c for AuGe/Ni/Au contact is slightly lower after post-annealing for 1 h at 300 °C and for 1 min at 300 °C with 10 cycles than the value of 2.5×10^{-5} Ω·cm^2 without post-annealing, while it decreases to 2.1×10^{-6} Ω·cm^2 after post-annealing at 490 °C for 15 min. These results demonstrate that the AuGe/Ni/Au contact presents a lower ρ_c compared with the Ti/Au contact and a higher post annealing temperature is more effective to decrease the ρ_c.

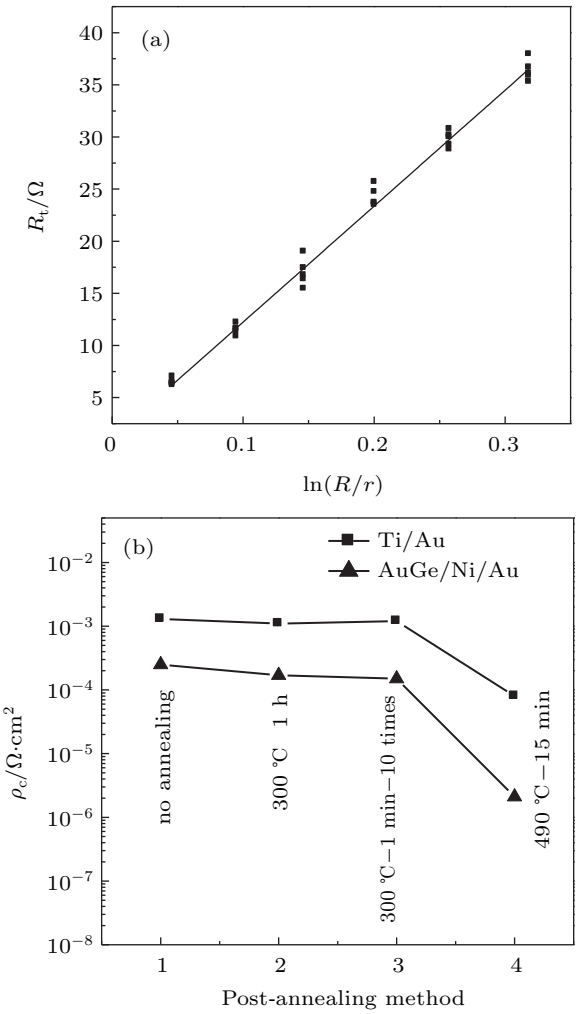


Fig. 2. (a) Resistance of each circular as a function of $\ln(R/r)$ and the linear fitting for AuGe/Ni/Au–graphene contact post-annealed at 490 °C for 15 min. (b) Post-annealing method effects on specific contact resistivity (ρ_c) for Ti/Au and AuGe/Ni/Au contacts without pre-annealing.

Figure 3 shows the dependence of ρ_c on the post-annealing temperature for Ti/Pt/Au– and AuGe/Ni/Au–graphene contacts without pre-annealing. The ρ_c for Ti/Pt/Au–graphene contact drops 89.7% from 3.0×10^{-4} Ω·cm^2 to 3.1×10^{-5} Ω·cm^2 by post-annealing at 400 °C for 15 min, and then it increases to 8.2×10^{-5} Ω·cm^2 after post-annealing at 490 °C for 15 min. While for AuGe/Ni/Au

contact, the ρ_c is 2.1×10^{-6} Ω·cm^2 after post-annealing at 490 °C for 15 min which is 2 orders of magnitude lower than that without post-annealing, and it is lower than that for Ti/Pt/Au contact post-annealed at 400 °C, suggesting a better ohmic contact using AuGe/Ni/Au compared with Ti/Pt/Au.

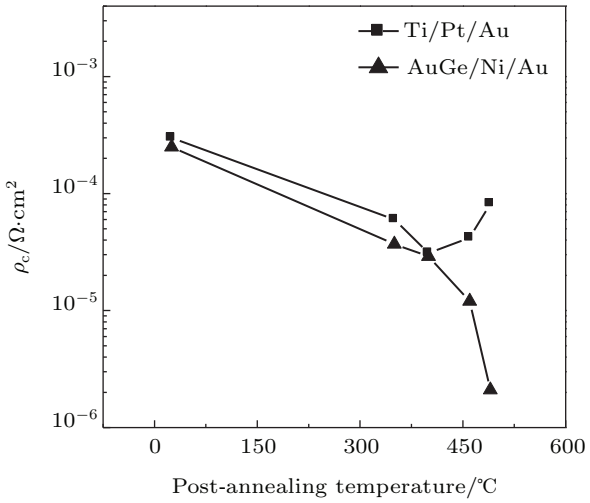


Fig. 3. Measured ρ_c for Ti/Pt/Au– and AuGe/Ni/Au–graphene contacts post-annealed at various temperatures for 15 min.

Figure 4(a) shows the ρ_c versus post-annealing temperature for AuGe/Ni/Au–graphene contacts without pre-annealing and pre-annealed at 200 and 300 °C for 1 h. Before post-annealing, the ρ_c of the contact without pre-annealing is 2.5×10^{-4} Ω·cm^2, and it decreases significantly to 2.1×10^{-6} Ω·cm^2 when the contact was post-annealed at 490 °C for 15 min. However, the ρ_c increases to 6.8×10^{-6} Ω·cm^2 when the contact was annealed at 550 °C for 15 min. The contact pre-annealing at 200 and 300 °C for 1 h facilitates a much more substantial drop in ρ_c compared with that without pre-annealing, which results from the significant removal of residues by a high temperature. Thus, the lowest ρ_c is achieved when the contact is pre-annealed at 300 °C for 1 h and post-annealed at 490 °C for 15 min. Further results of the improved ρ_c by optimizing the post-annealing time are shown in Fig. 4(b). The contact post-annealed at 490 °C for 60 s yields nearly a 98.8% reduction in ρ_c compared with the contact without post-annealing. While further increasing in the post-annealing time for the contact from 60 s to 900 s leads to a gradual increase in ρ_c from 9.5×10^{-7} Ω·cm^2 to 2.1×10^{-6} Ω·cm^2

A lot of work has been done to investigate the metal–graphene contacts. Residues on graphene, the contact area pattern of graphene under metal, and contact area between metal and graphene can modify the contact resistance.[7,10,19] Furthermore, doping of graphene by metal depends on the metal species and chemisorption of metal on graphene because of small equilibrium separations and large binding energies together contribute to the contact resistance.[11,21,22] The ρ_c for Ti/Au, Ti/Pt/Au and AuGe/Ni/Au contacts shown in Figs. 2(b) and 3 all decrease after post-annealing at high temperatures, which is mainly due to the formations of strong bonding such as the TiC and GeC at the metal/graphene interface and the increased effective contact area between metal and graphene. Because Ti and Ge atoms are both chemisorbed on graphene and the effective contact area varies with the post-annealing temperature.[19,23–25] The work function of Ti (4.35 eV) is lower than that of graphene (4.5 eV), thus charge transfer occurs between the Ti and graphene to align the Fermi levels. This results in n-type doping of the graphene.[23] While Ge is the 4 p element that is embedded more easily in the sp^2 C framework which suggests a substantial further enhancement of n-type doping of graphene layers.[27] This may result in the relatively low ρ_c for AuGe/Ni/Au contact compared with that of Ti/Au and Ti/Pt/Au contacts.

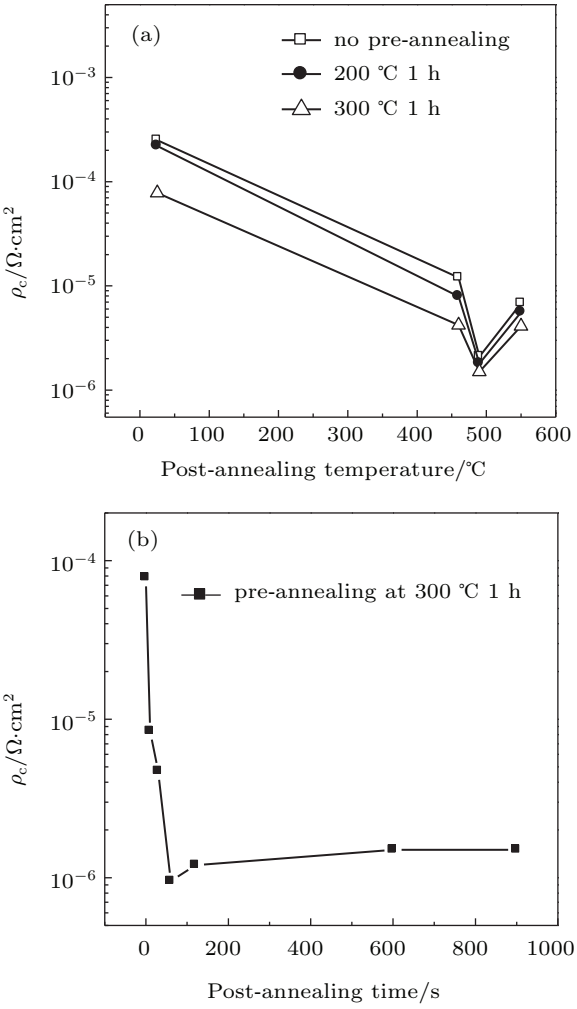


Fig. 4. Measured ρ_c as a function of (a) post-annealing temperature and (b) post-annealing time for AuGe/Ni/Au–graphene contact pre-annealed at 300 °C for 1 h.

In Fig. 3, the lowest ρ_c for the Ti/Pt/Au–graphene contact is obtained at 400 °C, since the Au penetrates through the Pt diffusion barrier and may lead to an enhanced Au–Ti intermatallic reaction and rapid formation of the α and β TiAu

phases with increasing annealing temperature.[28] This may lead to outward diffusion of Ti from graphene. As shown in Fig. 5, the Au surface is smoother after increasing the annealing temperature from 350 °C to 400 °C, while the surface morphology degrades dramatically after annealing at 460 °C and 490 °C, which is indicative of the interdiffusion and reaction of the Au cap layer with the Pt and Ti.

AuGe/Ni/Au shows different alloyed properties compared with Ti/Pt/Au contact. As Ni_3Ge is firstly alloyed after annealing at low temperature, upon heating, Ni and Ge are outdiffused from Ni_3Ge.[24] Thus, more GeC strong bonding which leads to low ρ_c can form with increasing annealing temperature. As shown in Fig. 6, the AuGe/Ni/Au contact surface is smoother as a result of increasing the annealing temperature from 400 °C to 460 °C, then pitting takes place after further increasing the annealing temperature from 490 °C to 550 °C. The variation of contact resistivity with alloy temperature for AuGe/Ni/Au was found to depend on the presence of these pittings.[24] Small dense pittings produce a lower contact resistivity, while big sparse pittings produce a higher contact resistivity. Thus, ρ_c decreases with increasing the annealing temperature from 460 °C to 490 °C, then it increases with increasing the annealing temperature to 550 °C. Annealing time is another parameter in the annealing process that affects the contact resistivity. Increasing annealing time may decrease the percentage of the Ge–graphene interface covered by GeC, since more Au and Ni may diffuse to the metal–graphene interface. Also increasing the annealing time can coarsen the pittings.[24] The reasons mentioned above can all lead to an increase in contact resistivity with long annealing time. Here the optimized annealing time for the AuGe/Ni/Au–graphene contact is 60 s.

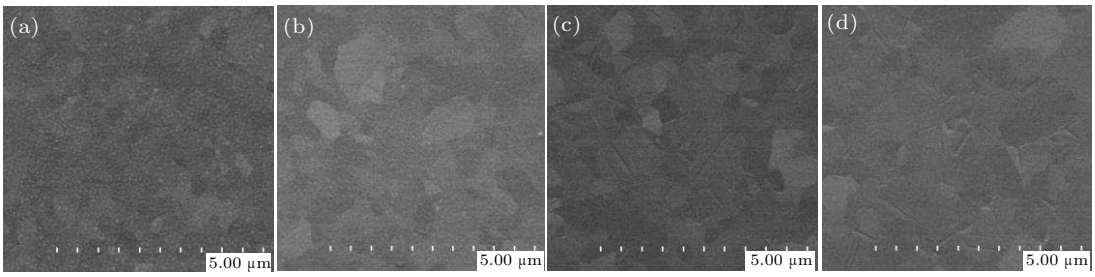


Fig. 5. SEM image of alloyed Ti/Pt/Au contact surface after annealing at (a) 350 °C, (b) 400 °C, (c) 460 °C, and (d) 490 °C for 15 min.

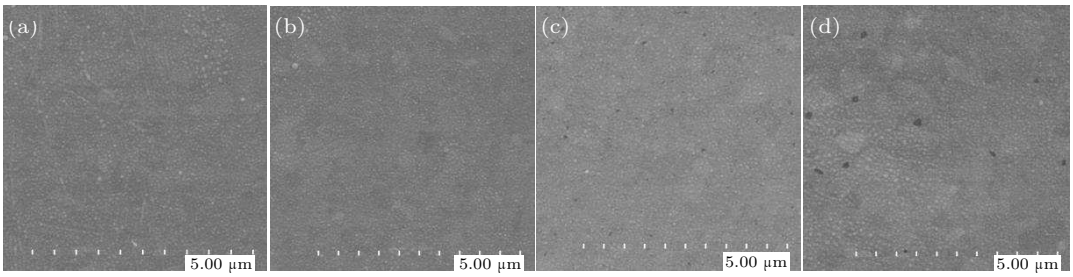


Fig. 6. SEM image of alloyed AuGe/Ni/Au contact surface after annealing at (a) 400 °C, (b) 460 °C, (c) 490 °C, and (d) 550 °C for 15 min.

4. Conclusion

In summary, by employing the AuGe/Ni/Au contact, the lower specific contact resistivity with graphene is obtained after thermal annealing compared with that of Ti/Au and Ti/Pt/Au contacts fabricated using the same process. It is necessary to pre-anneal the AuGe/Ni/Au–graphene contact at 300 °C for 1 h and post-anneal it at 490 °C for 60 s to obtain a specific contact resistivity of 9.5×10^{-7} Ω·cm^2. Experimental results indicate that AuGe/Ni/Au is a very good candidate for the ohmic contact metal with graphene. Low specific contact resistivity to graphene achieved by AuGe/Ni/Au and the annealing process may be combined with an edge-contact and therefore lays a foundation for further progress in graphene device performance.

References

[1] Tang C C, Li M Y, Li L J, Chi C C and Chen J C 2012 *Appl. Phys. Lett.* **101** 202104
[2] Miao X, Tongay S, Petterson M K, Berke K, Rinzler A G, Appleton B R and Hebard A F 2012 *Nano Lett.* **12** 2745
[3] Kim R H, Bae M H, Kim D G, Cheng H, Kim B H, Kim D H, Li M, Wu J, Du F, Kim H S, Kim S, Estrada D, Hong S W, Huang Y, Pop E and Rogers J A 2011 *Nano Lett.* **11** 3881
[4] Moon J S, Curtis D, Bui S, Hu M, Gaskill D K, Tedesco J L, Asbeck P, Jernigan G G, Van Mil B L, Myers-Ward R L, Eddy C R, Campbell P M and Weng X 2010 *IEEE Electron Dev. Lett.* **31** 260
[5] Fang Z, Liu Z, Wang Y, Ajayan P M, Nordlander P and Halas N J 2012 *Nano Lett.* **12** 3808

[6] Yang X X, Sun J D, Q H, Lv L, Su L N, Yan B, Li X X, Zhang Z P and Fang J Y 2015 *Chin. Phys. B* **24** 047206
[7] Huang J, Guo L W, Lu W, Zhang Y H, Shi Z, Jia Y P, Li Z L, Yang J W, Chen H X, Mei Z X and Chen X L 2016 *Chin. Phys. B* **25** 067205
[8] Balci O and Kocabas C 2012 *Appl. Phys. Lett.* **101** 243105
[9] Smith J T, Franklin A D, Farmer D B and Dimitrakopoulos C D 2013 *ACS Nano* **7** 3661
[10] Nath A, Koehler A D, Jernigan G G, Wheeler V D, Hite J K, Hernandez S C, Robinson Z R, Garces N Y, Myers-Ward R L, Eddy C R, Gaskill D K and Rao M V 2014 *Appl. Phys. Lett.* **104** 224102
[11] Song S M, Park J K, Sul O J and Cho B J 2012 *Nano Lett.* **12** 3887
[12] Robinson J A, LaBella M Zhu M, Hollander M, Kasarda R, Hughes Z, Trumbull K, Cavalero R and Snyder D 2011 *Appl. Phys. Lett.* **98** 053103
[13] Li W, Liang Y, Yu D, Peng L, Pernstich K P, Shen T, Hight Walker A R, Cheng G J, Hacker C A, Richter C A, Li Q, Gundlach D J and Liang X 2013 *Appl. Phys. Lett.* **102** 183110
[14] Lim Y D, Lee D Y, Shen T Z, Ra C H, Choi J Y and YooW J 2012 *ACS Nano* **6** 4410
[15] Leong W S, Nai C T and Thong J T L 2014 *Nano Lett.* **14** 3840
[16] Jang C W, Kim J H, Kim J M, Shin D H, Kim S and Choi S H 2013 *Nanotechnology* **24** 405301
[17] Cheng Z, Zhou Q, Wang C, Li Q, Wang C and Fang Y 2011 *Nano Lett.* **11** 767
[18] Moon J S, Curtis D, Hu M, Wong D, McGuire C, Campbell P M, Jernigan G, Tedesco J L, Van Mil B, Myers-Ward R, Eddy C and Gaskill D K 2009 *IEEE Electron Dev. Lett.* **30** 650
[19] Ito K, Ogata T, Sakai T and Awano Y 2015 *Appl. Phys. Express* **8** 025101
[20] Wang L, Zhang Y, Li X, Liu Z, Guo E, Yi X, Wang J, Zhu H and Wang G 2012 *J. Phys. D: Appl. Phys.* **45** 505102
[21] Watanabe E, Conwill A, Tsuya D and Koide Y 2012 *Diam. Relat. Mater.* **24** 171
[22] Giovannetti G, Khomyakov P A, Brocks G, Karpan V M, van den Brink J and Kelly P J 2008 *Phys. Rev. Lett.* **101** 026803
[23] Gong C, McDonnell S, Qin X, Azcatl A, Dong H, Chabal Y J, Cho K and Wallace R M 2014 *ACS Nano* **8** 642
[24] Tahamtan S, Goodarzi A, Abbasi S P, Hodaei A, Zabihi M S and Sabbaghzadeh J 2011 *Microelectr. Reliab.* **51** 1330
[25] Aktürk E, Ataca C and Ciraci S 2010 *Appl. Phys. Lett.* **96** 123112
[26] Khomyakov P A, Giovannetti G, Rusu P C, Brocks G, van den Brink J and Kelly P J 2009 *Phys. Rev. B* **79** 195425
[27] Denis P A 2014 *Chem. Phys. Chem.* **15** 3994
[28] Katz A, Weir E and Dautremont-Smith W C 1990 *J. Appl. Phys.* **68** 1123